Field Solution for Radial Waveguides with Annular Discontinuities

BAHMAN AZARBAR, MEMBER, IEEE, AND LOTFOLLAH SHAFAI

Abstract—**A method is established which gives the internal field of a radial waveguide in the presence of annular-type slots on the conducting walls or metallic scatterers inside the guide. The exciting field can have a general form, and the dielectric constant of the region could be lossy or lossless. To obtain a solution, the induced currents (magnetic current in case of slot-type discontinuity) over the scattering bodies are expanded into a finite series of suitable basis functions with unknown coefficients. The total number of these functions is directly related to the electrical dimensions of the scatterers. The complex coefficients are then obtained by employing the appropriate Green's functions and an application of the boundary conditions over the scattering bodies. The method is then applied to the problem of coupling between two radials waveguides by annular slots on the common boundary. It is shown that in general, higher order modes have significant effect on the solution, and for a precise evaluation of the field their contribution must also be included.**

I. Introduction

TWO-DIMENSIONAL arrangement of slots or conducting plates to form resonant arrays are of practical interest for applications such as bandpass or bandstop filters. Within a certain frequency band the transmission coefficient of the array can vary from unity to zero and its resonance frequency and bandwidth may be controlled by varying the characteristic dimensions of the array [1]–[3].

So far, the subject matter is investigated extensively for the cases where the basic array element has rectangular, circular, or cross-shape geometries. However, little information is available for the case where the scattering body is of annular shape.

In the present work, using a boundary value treatment, a method of solution is established which gives the interior field of a radial waveguide containing annular slots on its surface or annular metallic plates within the guide structure. A solution for the case in which both type of discontinuities are present can simply be obtained by superposing the two set of solutions. The application of the boundary conditions over the slots and the conducting bodies for determining the currents (electric and magnetic) then ensures the electromagnetic coupling between the two set of solutions. The exciting source is placed at the center of the radial waveguide and its field may be of a general nature. The slots and plates are assumed to be electrically thin enough as to suppress radially directed induced currents over them. Thus the induced surface currents (electric and magnetic) on the surfaces of the array elements are in the azimuthal direction.

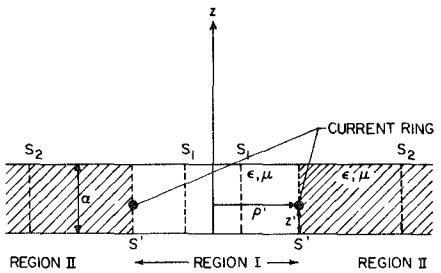

Fig. 1. Current ring in a radial waveguide (impulse response).

We develop the solution by first constructing appropriate Green's functions describing the impulse response to an electric (or magnetic) current ring of strength I located at $\rho=\rho'$, Fig. 1. The final formulation of the problem is then obtained by an integration of the impulse response over the induced source distribution (surface of the scatterer). Depending on the electrical dimension of the element, the induced current may be expressed in terms of a finite sum of a suitable set of basis functions with unknown coefficients. These constants are then obtained by an application of the boundary conditions over the surface of the scatterer. Depending on the required degree of accuracy of the solution and the electrical width of each element, the induced current can be represented by variety of expressions [4]. For electrically narrow slots (or plates), current distribution over each element may be assumed to be constant with respect to ρ. In fact, Wait and Hill [5], [6], by considering the problem of TEM coupling by a circumferential slot on a coated coaxial cable, have shown that differences between the results of higher order approximations for the aperture field distribution and the constant field model are inconsequential. Thus using the constant field approximation, each element of the array is characterized by a complex constant which is yet to be determined by an application of the boundary conditions.

For a waveguide-fed slot array, Fig. 2, in which apertures are fed successively by a traveling wave, the effect of the mutual coupling among the slots cannot be generally ignored. In the methods based on the waveguide transmis-

Manuscript received December 5, 1977; revised November 20, 1978. This paper was supported by the National Research Council of Canada under Grant A7702, and the Department of Electrical Engineering, University of Manitoba, Winnipeg, Canada.

B. Azarbar is with the System Engineering Department, Telesat Canada, Ottawa, Ont., Canada.

L. Shafai is with the Department of Electrical Engineering, University of Manitoba, Winnipeg, Man., Canada R3T 2N2.

0018-9480/79/1100-0883$00.75 ©1979 IEEE

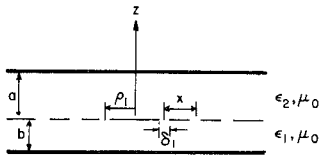

Fig. 2. Two typical coupled radial waveguides of infinite extent.

sion-line concept, the coupling between the array elements is usually accounted for only the dominant propagating mode, that is, totally ignoring the effects of higher order modes created in the vicinity of the slot discontinuities. Furthermore, the coupling due to the external field is generally overlooked. However, as it will be shown later, depending on the arrangement of the slots and their electrical dimensions, the external coupling can become so strong as to recouple part of the radiated power back into the guide containing the exciting source. An equivalent transmission-line representation then gives a negative radiation conductance for the respective member (or members) of the array. The contribution of the higher order modes can also become appreciable as to turn a resonant slot, when radiating by itself, into a reactive element. A distinct advantage of the present approach is the fact that all mutual coupling effects and the higher order modes are incorporated automatically in the solution. This is achieved by the simultaneous evaluation of the field unknown coefficients through the application of the boundary conditions.

II. Problem Formulation and Solution

A. Constuction of Green's Functions, Magnetic Ring

In deriving the appropriate Green's functions for the problem depicted in Fig. 1, we essentially follow a similar approach taken by Collin [7] in which field radiated by a current filament in a cylindrical waveguide is derived for the case when propagation is taken place in a cylindrical tube. The basic principle is to expand the radiated field in terms of a suitable set of waveguide modes with unknown coefficients. These coefficients are then determined by an application of the Lorentz Reciprocity theorem.

Consider the geometry shown in Fig. 1 formed by a radial waveguide of thickness a. The constitutive parameters of the medium between the perfectly conducting planes are ϵ and μ. We assume the guide is infinite extent in the ρ direction, resulting in a zero reflection coefficient. In practice a matched load may simulate this condition. The source is a magnetic filament of strength $I_m(\phi)$, characterized by

$$\vec{J}_m(\phi) = I_m(\phi)\delta(\rho-\rho')\delta(z-z')\hat{\phi}' \tag{1}$$

where $I_m(\phi)$ is a general continuous function of the azimuthal angle ϕ and ρ' and z' are the coordinates of the source. A time variation of $\exp(j\omega t)$ is assumed and suppressed throughout. The source function may be expanded in a Fourier series of the form:

$$I_m(\phi) = \sum_{n=0}^{\infty} (a_n \cos n\phi + b_n \sin n\phi), \qquad 0 \leqslant \phi \leqslant 2\pi \tag{2}$$

where a_n and b_n are the Fourier coefficients. The source singularity at $\rho=\rho'$ and $z=z'$ suggests dividing the region inside the guide into two regions separated by the source plane S', namely, region I for $\rho<\rho'$ and region II for $\rho'<\rho$. Considering the finiteness of the fields in region I and the radiation condition in region II would lead us to the following expressions for the wave functions:

$$\Psi^e = \sum_{n=0}^{\infty}\sum_{m=0}^{\infty} (a_n \cos n\phi + b_n \sin n\phi) \cdot \cos\left(\frac{m\pi}{a} z\right) \begin{cases} u^e_{mn} J_n(k_{\rho m}\rho), & \rho<\rho' \\ U^e_{mn} H^{(2)}_n(k_{\rho m}\rho), & \rho>\rho' \end{cases} \tag{3}$$

$$\Psi^h = \sum_{n=0}^{\infty}\sum_{m=0}^{\infty} n(b_n \cos n\phi - a_n \sin n\phi) \cdot \sin\left(\frac{m\pi}{a} z\right) \begin{cases} u^h_{mn} J_n(k_{\rho m}\rho), & \rho<\rho' \\ U^h_{mn} H^{(2)}_n(k_{\rho m}\rho), & \rho>\rho' \end{cases} \tag{4}$$

where the subscripts e and h refer to the TM and TE fields, respectively, and

$$k_{\rho m} = \left[k^2 - \left(\frac{m\pi}{a}\right)^2\right]^{1/2}$$
$$k = \omega\sqrt{\epsilon\mu}\ . \tag{5}$$

An application of the Lorentz Reciprocity theorem [8] to a volume V bounded by the conducting plates and two arbitrarily located cylindrical surfaces S_1 and S_2 in regions I and II, respectively, leads to

$$\iint_S (\vec{E}_a \times \vec{H} - \vec{E} \times \vec{H}_a)\cdot\hat{n}\, ds = \int_V (\vec{H}\cdot\vec{J}_{am} - \vec{E}\cdot\vec{J}_a - \vec{H}_a\cdot\vec{J}_m)\, dv \tag{6}$$

where the subscript a represents the auxiliary fields and their sources, $\hat{n}$ is the inward unit normal of the closed boundary S, and $\vec{J}_m$ is given by (1) and (2). In (6), as long as the auxiliary fields satisfy the Maxwell's equations, we are free to select their form to facilitate the derivation of the solution. We, therefore, choose two separate sets of modes, where each set consists of two single modes of TE and TM types which are the solutions of the source free-wave equations in volume V. Hence,

$$\begin{cases} \Psi^e_a = (a_l \cos l\phi + b_l \sin l\phi)\cos\left(\dfrac{p\pi}{a} z\right) J_l(k_{\rho p}\rho) \\ \Psi^h_a = l(b_l \cos l\phi - a_l \sin l\phi)\sin\left(\dfrac{p\pi}{a} z\right) J_l(k_{\rho p}\rho) \end{cases} \tag{7a}$$

$$\begin{cases} \Psi^e_a = (a_l \cos l\phi + b_l \sin l\phi)\cos\left(\dfrac{p\pi}{a} z\right) H^{(2)}_l(l_{\rho p}\rho) \\ \Psi^h_a = l(b_l \cos l\phi - a_l \sin l\phi)\sin\left(\dfrac{p\pi}{a} z\right) H^{(2)}_l(k_{\rho p}\rho). \end{cases} \tag{7b}$$

Taking the auxiliary wave functions represented by (7a) and after some algebraic manipulation, (6) is transformed

to the following form:

$$\left[l^2\epsilon U^h_{pl}-\mu U^e_{pl}\right]=-\frac{\omega\epsilon\mu\epsilon_p\pi}{2ak^2_{\rho p}}\cos\left(\frac{p\pi}{a}z'\right)\left[\rho' k_{\rho p}J_l'(k_{\rho p}\rho)-l^2\frac{p\pi}{j\omega\mu a}J_l(k_{\rho p}\rho')\right]. \quad (8a)$$

Similarly, substituting (7b) in (6) leads to

$$\left[l^2u^h_{pl}-\mu u^e_{pl}\right]=-\frac{\omega\epsilon\mu\epsilon_p\pi}{2ak^2_{\rho p}}\cos\left(\frac{p\pi}{a}z'\right)\left[\rho' k_{\rho p}H_l^{(2)\prime}(k_{\rho p}\rho')-l^2\frac{p\pi}{j\omega\mu a}H_l^{(2)}(k_{\rho p}\rho')\right] \quad (8b)$$

where use has been made of the Wronskian relations for the Bessel's functions, and

$$\epsilon_p=\begin{cases}1, & p=0\\ 2, & p\neq 0.\end{cases} \quad (9)$$

Two other equations in terms of the unknown coefficients are needed to uniquely specify the field components inside the guide. To this end, we utilize the continuity of the axial components of the electric and the magnetic fields across the source plane S'. The continuity of the magnetic field yields

$$H_z^{\mathrm{I}}-H_z^{\mathrm{II}}=\frac{1}{j\omega\mu}\sum_{n=0}^{\infty}\sum_{m=0}^{\infty}n(b_n\cos n\phi-a_n\sin n\phi)\cdot k^2_{\rho m}\sin\left(\frac{m\pi}{a}z\right)\left[U^h_{mn}H_n^{(2)}(k_{\rho m}\rho')-U^h_{mn}J_n(k_{\rho m}\rho')\right]=0, \qquad \rho=\rho',\quad 0\leqslant\phi<\pi. \quad (10a)$$

Using the orthogonality relations for the z and ϕ coordinates, one finds

$$U^h_{pl}H_l^{(2)}(k_{\rho p}\rho')-U^h_{pl}J_l(k_{\rho p}\rho')=0. \quad (10b)$$

The axial component of the electric field is discontinuous across the source plane S' by an amount equal to the surface magnetic-current density, i.e., $E_z^{\mathrm{II}}-E_z^{\mathrm{I}}=I_m(\phi)\delta(z-z')$, for $\rho=\rho'$ and $0\leqslant\phi\leqslant 2\pi$, which after simplification gives

$$\left[U^e_{pl}H_l^{(2)}(k_{\rho p}\rho')-U^e_{pl}J_l(k_{\rho p}\rho')\right]=\frac{j\omega\epsilon\cos\left(\frac{p\pi}{a}z'\right)}{k^2_{\rho p}a}\epsilon_p \quad (11)$$

(8a), (8b), (10b), and (11) constitute a set of equations for the determination of the unknown coefficients. Utilizing the Wronskian relationship of the Bessel functions one obtains

$$U^e_{mn}=\frac{\pi\omega\epsilon\rho'\cos\left(\frac{m\pi}{a}z'\right)}{2k_{\rho m}a}\epsilon_m J_n'(k_{\rho m}\rho')$$

$$u^e_{mn}=\frac{\pi\omega\epsilon\rho'\cos\left(\frac{m\pi}{a}z'\right)}{2k_{\rho m}a}\epsilon_m H_n^{(2)\prime}(k_{\rho m}\rho')$$

$$U^h_{mn}=-j\frac{m\pi^2\cos\left(\frac{m\pi}{a}z'\right)}{2(k_{\rho m}a)^2}\epsilon_m J_n(k_{\rho m}\rho')$$

$$u^h_{pl}=-j\frac{m\pi^2\cos\left(\frac{m\pi}{a}z'\right)}{2(k_{\rho m}a)^2}\epsilon_m H_n^{(2)}(k_{\rho m}\rho'). \quad (12)$$

Equations (1)–(4) and (12) uniquely define the field of a magnetic-current filament located at (ρ',z') inside a radial waveguide.

B. Construction of Green's Functions, Electric Ring

The mathematical routine for deriving the appropriate Green's functions for the case of an electric-current filament is similar to that of the magnetic case. For the sake of brevity only the main differences together with the final result will be presented. Aside from subscript m, the defining equations for the current density and its Fourier expansion are the same as (1) and (2). Hence, the required wave functions are given by

$$\Psi^e=\sum_{n=0}^{\infty}\sum_{m=0}^{\infty}n(b_n\cos n\phi-a_n\sin n\phi)\cdot\cos\left(\frac{m\pi}{a}z\right)\begin{cases}u^e_{mn}J_n(k_{\rho m}\rho), & \rho<\rho'\\ U^e_{mn}H_n^{(2)}(k_{\rho m}\rho), & \rho>\rho'\end{cases} \quad (13a)$$

$$\Psi^h=\sum_{n=0}^{\infty}\sum_{m=0}^{\infty}(a_n\cos n\phi+b_n\sin n\phi)\cdot\sin\left(\frac{m\pi}{a}z\right)\begin{cases}u^h_{mn}J_n(k_{\rho m}\rho), & \rho<\rho'\\ U^h_{mn}H_n^{(2)}(k_{\rho m}\rho), & \rho>\rho'.\end{cases} \quad (13b)$$

The reciprocity relation for this case is

$$\iint_S(\vec{E}_a\times\vec{H}-\vec{E}\times\vec{H}_a)\cdot\hat{n}\,ds=\int_V\vec{E}_a\cdot\vec{J}\,d_v. \quad (14)$$

Using these relations, one finds

$$\left[\epsilon U^h_{pl}-l^2\mu U^e_{pl}\right]=\frac{\pi\omega\epsilon\mu}{ak^2_{\rho p}}\sin\left(\frac{p\pi}{a}z'\right)\left[k_{\rho p}J_l'(k_{\rho p}\rho')+\frac{l^2p\pi}{j\omega\epsilon\rho' a}J_l(k_{\rho p}\rho')\right] \quad (15a)$$

$$\left[\epsilon u^h_{pl}-l^2\mu u^e_{pl}\right]=\frac{\pi\omega\mu}{ak^2p\rho}\sin\left(\frac{p\pi}{a}z'\right)\left[k_{p\rho}H_l^{(2)\prime}(k_{\rho p}\rho')+\frac{l^2p\pi}{j\omega t\rho' a}H_l^{(2)}(k_{\rho p}\rho')\right]. \quad (15b)$$

Now, in contrast to the first case, the axial component of the electric field E_z is continuous across the source plane s', but H_z is discontinuous by an amount equal to

$$H_z^{\mathrm{I}}-H_z^{\mathrm{II}}=I(\phi)\delta(z-z'), \qquad \rho=\rho',\quad 0\leqslant\phi<2\pi. \quad (16)$$

Using these conditions and similar steps as the previous

case, one finds

$$U^e_{mn}=j\frac{m\pi^2\sin\left(\frac{m\pi}{a}z'\right)}{(k_{\rho m}a)^2}J_n(k_{\rho m}\rho')$$

$$u^e_{mn}=j\frac{m\pi^2\sin\left(\frac{m\pi}{a}z'\right)}{(k_{\rho m}a)^2}H^{(2)}_n(k_{\rho m}\rho')$$

$$U^h_{mn}=-\frac{\pi\omega\mu\rho'\sin\left(\frac{m\pi}{a}z'\right)}{k_{\rho m}a}J'_n(k_{\rho m}\rho')$$

$$u^h_{mn}=-\frac{\pi\omega\mu\rho'\sin\left(\frac{m\pi}{a}z'\right)}{k_{\rho m}a}H^{(2)\prime}_n(k_{\rho m}\rho') \qquad (17)$$

which completes the determination of the Green's functions for this case. The field setup by any combination of sources of electric and magnetic type may be looked upon as a superposition problem.

Based on the theory presented, the next section is devoted to the demonstration of the application of the previous results to problems involving annular slots of finite widths. To show the general feature of the theory, the problem of coupling between two radial waveguides by annular apertures on the common boundary is considered, Fig. 2. The exciting source is placed in the central region of the lower waveguide.

The solution of the problems involving annular or cylindrical metallic plates as the scatterers of electromagnetic fields inside a radial waveguide can be obtained in a similar manner. That is, using the appropriate Green's functions of electric type developed earlier, the solution can be obtained by integrating the impulse response over the induced current distributed over the surfaces of the conductors. The unknown coefficients are then determined by applying the condition of vanishing tangetial electric field on the surfaces of the conducting objects. These geometries may have applications as bandpass filters, and also be used for the design of feed systems suitable for launching a particular mode or modes for use in radial waveguides.

III. Formulation of Two Coupled Radial Waveguides

An annular slot on the conducting wall of a radial waveguide may be viewed as an annular distribution of magnetic surface current with a density given by

$$\vec{J}_m(\rho',\phi',z')=\vec{E}\times\hat{n}|\,\text{aperture} \qquad (18)$$

where $\hat{n}$ is the inward unit vector normal to the aperture plane. Considering the fact that E_ϕ component of the electric field must vanish at the edges of the slot, it is expected that for electrically narrow slots, the contribution from E_ϕ to the total field be negligible. Hence, we assume the aperture electric field to be mainly in the radial direction, that is,

$$\vec{J}_{ms}(\rho',\phi',z')\simeq E_\rho[\hat{\rho}\times\hat{n}]. \qquad (19)$$

Expanding the radial component of the electric field into a Fourier series of the azimuthal variable ϕ leads to

$$E_\rho(\rho,\phi)=\sum_{n=0}^{\infty}f_n(\rho)(a_n\cos n\phi+b_n\sin n\phi) \qquad (20)$$

where $f_n(\rho)$ is the radial dependent part of the aperture electric field. Now, the scattered field due to the slot can be obtained from the integral of the product of $f_n(\rho)$ and the wave functions over the aperture. To be more specific, consider the geometry shown in Fig. 2 and assume a TM_{01} mode of the radial waveguide [8] to be incident from region I. This mode is characterized by

$$\Psi^{e^{\text{inc}}}_{01}=\cos\phi H^{(2)}_1(k_1\rho) \qquad (21)$$

where

$$k_1=\sqrt{\epsilon_1\mu}\,.$$

The scattered wave functions inside the two waveguides are specified by

$$\Psi^e_2=-\frac{\pi\omega\epsilon_2}{2a}\sum_{l=1}^{L}\sum_{m=0}^{\infty}\sum_{n=0}^{\infty}\frac{\epsilon_m}{k_{\rho m_2}}\cdot(a_n\cos n\phi+b_n\sin n\phi)\cos\frac{m\pi}{a}z\cdot\begin{bmatrix}H^{(2)}_n(k_{\rho m_2}\rho) & \int_{\rho_l-\frac{\delta l}{2}}^{\rho_l+\frac{\delta l}{2}}\rho' f_{l_n}(\rho')\,d\rho' & J'_n(k_{\rho m_2}\rho')\\ J_n(k_{\rho m_2}\rho) & & H^{(2)\prime}_n(k_{\rho p}\rho')_{m_2}\end{bmatrix}$$

$$\Psi^h_2=j\frac{\pi^2}{2a^2}\sum_{\rho=1}^{L}\sum_{m=0}^{\infty}\sum_{n=0}^{\infty}\frac{\epsilon_{m\cdot m\cdot n}}{k^2_{\rho m_2}}\cdot(b_n\cos n\phi-a_n\sin n\phi)\sin\frac{m\pi}{a}z\cdot\begin{bmatrix}H^{(2)}_n(k_{\rho m_2}\rho) & \int_{\rho_l-\frac{\delta l}{2}}^{\rho_l+\frac{\delta l}{2}}f_{l_n}(\rho')\,d\rho' & J_n(k_{\rho m_2}\rho')\\ J_n(k_{\rho m_2}\rho) & & H^{(2)}_n(k_{\rho m_2}\rho')\end{bmatrix} \qquad (22)$$

$$\Psi^e_1=\frac{\pi\omega\epsilon_1}{2b}\sum_{l=1}^{L}\sum_{m=0}^{\infty}\sum_{n=0}^{\infty}\frac{\epsilon_m}{k_{\rho m_1}}\cdot(a_n\cos n\phi+b_n\sin n\phi)\cos\frac{m\pi}{b}z\cdot\begin{bmatrix}H^{(2)}_n(k_{\rho m_1}\rho) & \int_{\rho_l-\frac{\delta l}{2}}^{\rho_l+\frac{\delta l}{2}}\rho' f_{l_n}(\rho')\,d\rho' & J'_n(k_{\rho m_1}\rho')\\ J_n(k_{\rho m_1}\rho) & & H^{(2)\prime}_n(k_{\rho m_1}\rho')\end{bmatrix}$$

$$\Psi_1^h = -j\frac{\pi^2}{2b^2}\sum_{l=1}^{L}\sum_{m=0}^{\infty}\sum_{n=0}^{\infty}\frac{\epsilon_m mn}{k_{\rho m_1}^2}\cdot(b_n\cos n\phi - a_n\sin n\phi)\sin\frac{m\pi}{b}z \cdot\begin{bmatrix} H_n^{(2)}(k_{\rho m_1}\rho) & \int_{\rho_l-\frac{\delta l}{2}}^{\rho_l+\frac{\delta l}{2}} J_n(k_{\rho m_1}\rho') \\ J_n(k_{\rho m_1}\rho) & f_{l_n}(\rho') \quad d\rho' \quad H_n^{(2)}(k_{\rho m_1}\rho') \end{bmatrix} \tag{23}$$

where L is the total number of slots, $f_{l_n}(\rho')$ is the radial dependent part of the electric field over the lth aperture, and depending on the observation point ($\rho > \rho'$ or $\rho < \rho'$) the top or bottom row of the Bessel functions must be selected. It should be noted that the change of the sign in the solutions is due to the opposite directions for the respective inward normals. The continuity condition for the tangential electric field over the apertures is already implemented in the solution by insertion of equal field distributions in the above two sets of wave functions. The last boundary condition yet to be satisfied is the continuity of the tangential component of the total magnetic field over the apertures. Before proceeding further it should be pointed out that the coefficients a_n and b_n depend entirely on the functional form of the azimuthal dependence of the incident field. An examination of the total tangential magnetic field over the apertures, and using the orthogonality relations for sinusoidal functions over the range of $0 \leqslant \phi < 2\pi$, reveal that for our particular choice of the incident mode (21), we have

$$\begin{cases} b_n = 0, & \text{for all } n \\ a_n = 0, & n \neq 1 \\ a_1 = 1, & n = 1. \end{cases} \tag{24}$$

This eliminates the infinite summation over n in (22) and (23). Generally $f_{l_n}(\rho')$ is not a known function. However, depending on the electrical widths of the slots, this aperture field distribution may be expressed in terms of a finite sum of a particular set of basis functions with unknown coefficients. These coefficients are then obtained by applying the boundary condition on the tangential magnetic field over the apertures. The crudest choice for the basis functions is the step approximation. That is, the tangential electric field is assumed to be constant with respect to ρ over an electrically thin segment (unit cell) of the aperture, characterized by a complex constant E_i. Therefore, the total number of unknown field coefficients is equal to the total number of the unit cells of the individual slots. Evaluation of these constants can be performed using the continuity condition of either H_ϕ or H_ρ. The extra boundary condition appearing here is the result of our previous assumption made on the tangential electric field. The E_ϕ component of this field was assumed to be negligible compared to E_ρ. In fact, it seems quite possible to construct an extra set of wave functions describing the contribution from a ρ directed magnetic-current distribution over the apertures. Then, following the same routine as for the case of the ϕ directed magnetic current, we can expand E_ϕ over the apertures in terms of a finite sum of the basis functions with complex unknown coefficients.

The second continuity condition can then be employed to determine these new unknown coefficients. However, for the present case, we assume the slots are electrically narrow and for determination of the unknown field coefficients we utilize only the continuity condition on the H_ϕ component of the total magnetic field over the apertures. The total number of the matching points equals the total number of the field coefficients resulting in a set of linear equations for the unknowns. In the following examples, the unit cells (segments) are distributed uniformly over the apertures and the matching points are located at the center of each cell.

As an equivalent, principal-mode circuit representation, it is often desired to associate an admittance to each slot on the conducting boundaries. Here, we define the current and the voltage of the ith slot as

$$I_i = 2\pi H_\phi(\rho_i, \phi_0)\rho_i$$
$$V_i = \int_{\rho_i-(\delta_i/2)}^{\rho_i+(\delta_i/2)} E_\rho(\rho', \phi_0)\,d\rho' \tag{25}$$

where ρ_i is the radius of the center of the slot and ϕ_0 is an azimuthal angle, for which the magnitude of E_ρ and H_ϕ are maximum. Then the admittance characterizing the ith slot is defined as

$$Y_i = I_i / V_i. \tag{26}$$

When the field of the slot is due to several modes in the waveguide the slot admittance can be defined, in a usual manner, to relate the slot transfer power to the slot voltage. The power transferred through the slot can be obtained by integrating the Poynting vector across the slot, whereas the slot voltage can again be obtained using (25). In such a case the power coupled through the ith slot is related to its admittance by

$$P_{i_{\text{coupled}}} = Y_i V_i. \tag{27}$$

In the present problem the coupled power and its associated admittance are positive, when the direction of power flow is from the lower waveguide into the upper one. A negative power indicates the return of the power from the upper waveguide into the lower one.

As a check on the accuracy of the numerical results, the balance of the power flow from the incident wave into the transmitted and the coupled waves is examined, and in all cases satisfactory results are obtained.

IV. Numerical Results and Discussion

Based on the theory presented in the earlier sections, the following cases are considered. The thickness of the guides are smaller than $\lambda/2$, therefore, only the dominant

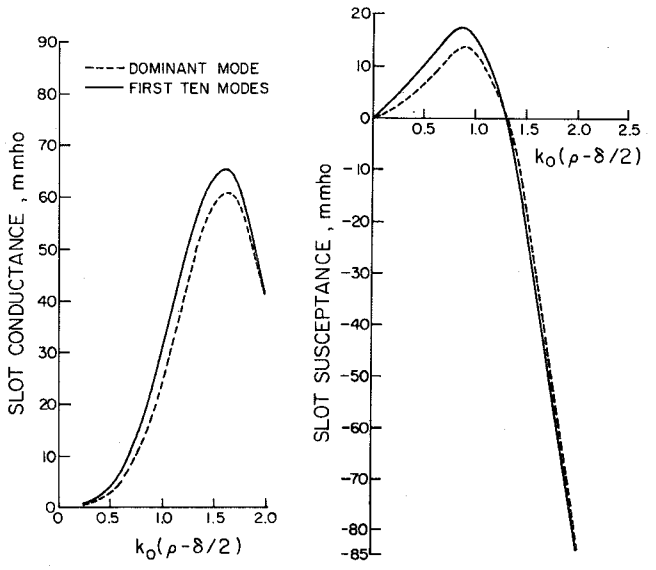

Fig. 3. The effect of higher order modes on the equivalent admittance of the slot. Ratio of the edges = 2.36, $k_0 b = k_0 a = 0.49$, $\epsilon_{r1} = \epsilon_{r2} = 1.00$. k_0 is free-space propagation constant.

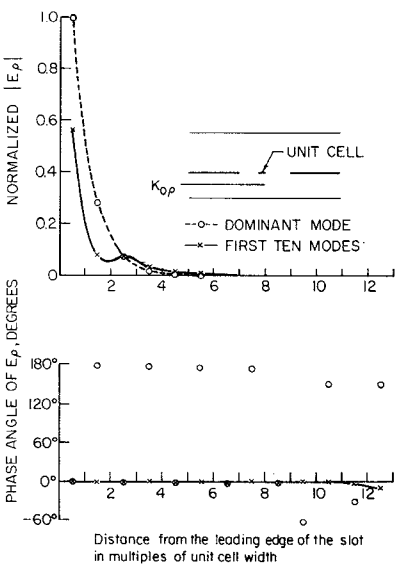

Fig. 4. Field distribution over the slot; $k_0\delta = 2.72$, $k_0\rho = 3.36$, $k_0 a = k_0 b = 0.49$, $\epsilon_{r1} = \epsilon_{r2} = 1.00$.

mode propagates. Fig. 3 depicts the variation of the conductance and the susceptance of a single slot as a function of the radius ρ of its inner edge. The ratio of the radii of the slot edges is kept constant and equal to 2.36. A TM_{00} excitation is assumed. The dotted lines in Fig. 3 represent the results obtained by taking only the propagating mode, whereas the solid lines are due to the inclusion of the first ten modes which was observed to be sufficient to yield a convergent solution for all the examples presented in this work. These results indicate that for most applications the dominant-mode representation, such as that in the transmission-line theory, adequately describes the slot admittance. However, the accuracy of the results, especially for central slots where $k\rho$ is small, is not satisfactory. As a further check on the dominant-mode approximation, the field distribution over the slot is also calculated, and is shown in Fig. 4. The slot is located at a radial distance $k(\rho - \delta/2) = 2.00$, which corresponds to the last plotted point of Fig. 3. Comparing the results one notes that the dominant-mode theory yields reasonable results for the field magnitude, except in the vicinity of the slot's leading edge. On the other hand, it fails to describe the phase of the field accurately. The actual phase of the slot field, which is calculated by including higher order modes excited by the slot discontinuity, is virtually constant across the slot, whereas the result due to the dominant mode oscillates between 0 and π for adjacent matching points. For these calculations the slot is divided into 13 cells (annular rings) of equal width and the field over each cell is computed by applying the continuity of the tangential magnetic field at its center. These calculations also show that the field distribution of an annular slot is similar to the current distribution on a conducting strip illuminated by a plane wave, [9]. It should also be noted that even though the dominant-mode approximation gives inaccurate phase distribution, it yields a reasonably accurate result for the equivalent slot voltage defined in (25). This is due to the fact that the equivalent slot voltage depends on the integral of the slot field and the phase oscillation compensates for inaccuracies in the slot-field amplitude. As a result, the slot admittance calculated by the dominant mode alone has reasonable accuracy.

TABLE I
CONTRIBUTION OF EACH SLOT TO THE TOTAL POWER COUPLED INTO THE GUIDE NUMBER TWO

SLOT NO.	POWER COUPLED BY EACH SLOT (PERCENTAGE OF TOTAL POWER)
1	+ 8.49
2	+ 2.11
3	- 23.32
4	- 2.77
5	+ 52.00
TOTAL COUPLED POWER	+ 36.51

$N = 5$ $\quad k_0\rho_1 = 4.00$
$\epsilon_{r_1} = 2.55$ $\quad k_0 x = 2.00$
$\epsilon_{r_2} = 1.00$ $\quad k_0 a = 0.25$
$k_0\delta = 0.20$ $\quad k_0 b = 0.49$

Table I is intended to show the strong coupling which exists between the two regions. Five annular slots of widths $k_0\delta = 0.20$ and separated by a distance $k_0 x = 2.00$ couple the two radial waveguides. Since the slots are electrically narrow, the calculations are carried out by representing each slot by a single cell. That is, each slot is characterized by a constant complex field E_i which is found by matching the field at its center. The results for the coupled power by individual slots show that the external coupling is strong and causes the return of a por-

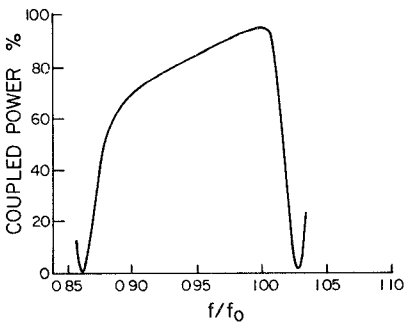

Fig. 5. Coupling characteristic of a single-slot TM_{00} exciting mode; $\epsilon_{r1}=2.60$, $\epsilon_{r2}=5.20$, $k_0a=0.34$, $k_0b=0.04$, $k_0\delta=0.05$, $k_0\rho=8.39$. All dimensions are at f_0.

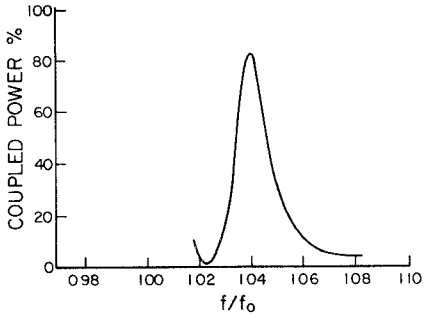

Fig. 6. Coupling characteristic of a four-slot TM_{00} exciting mode; $\epsilon_{r}2=5.20$, $\epsilon_{r1}=2.60$, $k_0a=k_0b=0.34$, $k_0\delta=0.08$, $k_0\rho_1=10.08$, $k_0x=4.05$.

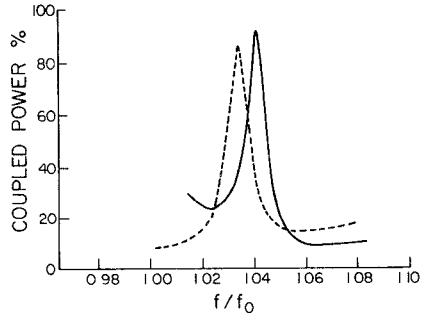

Fig. 7. Coupling characteristic of the geometry of Fig. 6 to TM_{01} mode of operation. The dotted curve is due to a 4-percent increase in slot spacing k_0x.

tion of the coupled power back to the exciting guide through the slots 3 and 4. An equivalent transmission-line representation is then a negative slot conductance (a source) associated with the respective slots.

Here, the power coupled by each slot is evaluated by an integration of the Poynting vector over the slot's surface. A positive power then indicates a power transfer from the lower waveguide into the upper one. The coupled power is negative when the integration gives a negative value, meaning a transfer of power from the upper waveguide into the lower one. Since the upper waveguide is assumed infinite in size, the coupled power propagates outward in that waveguide.

Figs. 5–7 show the coupling characteristics of annular slot arrays. The coupling characteristic of a single slot excited by a TM_{00} radial mode is shown in Fig. 5. It is interesting to note that by a proper selection of the geometry a single narrow slot can effectively couple a major part of the total power into the upper guide, over a wide-frequency band with a sharp cutoff characteristic.

Fig. 6 illustrates the coupling characteristic of four slots for a TM_{00} excitation. The characteristic of the same geometry with a TM_{01} excitation is shown in Fig. 7. The resonance peak is slightly shifted towards the higher frequencies and the bandwidth is decreased compared to TM_{00} mode of operation. This figure also shows the sensitivity of the coupling characteristic to the slot spacing. The dotted curve is obtained by increasing the spacing by an amount of 4 percent.

V. Summary and Conclusions

Using a boundary-value treatment a method of solution is established, which gives the field expressions inside a radial waveguide in the presence of annular-type slots on the conducting walls or metallic plates inside the guide. The expressions are general and can be used to determine the induced currents (electric or magnetic) by accurately matching the field over the slots or plates and a numerical solution of the resulting matrix equation. The scattering bodies, however, are assumed to be electrically narrow and the induced currents (electric or magnetic) are, therefore, in the azimuthal direction. The method also takes care of the mutual coupling among the slots or the plates. The exciting field can have a general form which may be assumed as a combination of the radial waveguide modes.

In application of the method to two coupled radial waveguides by an array of annular slot of finite width, it is shown that higher order modes may have significant effect on the solution and for a reasonably accurate solution their contribution must also be included. For most applications, however, the dominant-mode representation yields results with a reasonable degree of accuracy for the equivalent admittance characterizing each slot. The coupling characteristic of the geometry was also studied and it was shown that by a proper selection of the slot geometry and their arrangement in the array, wide or narrow bandpass characteristics can be obtained.

We, therefore, conclude that due to the inherent high-frequency capability of the waveguide structures and the simplicity of the present model such annular-slot arrays may be used in stripline circuits as a filter or coupler for dual feed systems. A thorough study of the slot admittance and its relation to the filtering characteristics is presently under investigation.

References

[1] R. B. Kieburtz and A. Ishimaru, "Scattering by a periodically apertured conducting screen," *IRE Trans. Antennas Propagat.*, vol. AP-9, pp. 506–514, Nov. 1961.

[2] R. H. Ott, R. G. Kouyoumjian, and L. Peters, Jr., "Scattering by a two-dimensional periodic array of narrow plates," *Radio Sci.*, vol. 2, pp. 1347–1349, Nov. 1967.

[3] C. C. Chen, "Transmission through a conducting screen perforated

periodically with apertures," *IEEE Trans. Microwave Theory Tech.*, vol. MTT-18, pp. 627–632, Sept. 1970.
[4] R. A. Hurd, "The field in a narrow circumferential slot in a coaxial waveguide," *Can. J. Phys.*, vol. 51, pp. 946–955, 1973.
[5] J. R. Wait and D. A. Hill, "On the electromagnetic fields of a dielectric coated coaxial cable," *IEEE Trans. Antennas Propagat.*, vol. AP-23, pp. 470–479, July 1975.
[6] ——, "Electromagnetic fields of a dielectric coated coaxial cable with interrupted shield-quasi-static approach," *IEEE Trans. Antennas and Propagat.*, vol. AP-23, pp. 679–682, Sept. 1975.
[7] R. E. Collin, *Field Theory of Guided Waves*. New York: McGraw-Hill, 1960, pp. 200–204.
[8] R. F. Harrington, *Time-Harmonic Electromagnetic Fields*. New York: McGraw-Hill, 1961, chs. 3–5, 1961.
[9] L. Shafai, "Currents induced on a conducting strip," *Can. J. Phys.*, vol 49, no. 4, pp. 495–498, 1971.

Time-Domain Analysis of Lumped-Distributed Networks

JAMES LAMAR ALLEN, FELLOW, IEEE

***Abstract*—A new method for time-domain analysis of networks containing transmission lines and lumped linear/nonlinear elements is presented. A key feature of the method is a procedure for generating a system matrix in a manner that involves only sums of subnetwork (or element) terms (no products or quotients). Numerical integration algorithms are used to reduce the problem to a solution of sparse algebraic equations.**

I. Introduction

TIME-DOMAIN analysis of lumped-element networks is well established. Powerful analytical and numerical techniques are readily available, including the popular state-space and Laplace transform methods. General purpose computer programs such as SCEPTRE [1] and SPICE [2] provide easy-to-implement time-domain solutions for complex lumped systems even when nonlinear, time-varying, and/or active elements are included.

The development of methods for transient analysis of mixed lumped-distributed networks is of relatively recent origin, and general techniques that permit, for example, lossy transmission lines of arbitrary lengths and nonlinear active lumped elements are not yet available. Yet, the time-domain analysis of such networks is increasingly important in design considerations of fast switching digital integrated circuits, broad-band radar and communication systems, time-domain reflectometry systems, and in the study of lightning and EMP effects in systems containing transmission lines, to mention only a few applications. The purpose of this paper is to present a technique suitable for the analysis of a very general class of lumped-distributed networks.

During the course of this study, a substantial literature search was carried out. The most pertinent articles and books are listed for the reader's convenience [3]–[17]. While the technique to be presented is significantly different from the methods found in the literature, the present concept grew from a "wouldn't it be nice if..." thought session following a May 21, 1976, reading of Silverberg's [3] paper. Since that time, the new technique has been successfully applied to a wide variety of problems. The impact of Silverberg's work is gratefully acknowledged.

Manuscript received April 12, 1979; revised August 21, 1979.
The author is with the University of South Florida, Tampa, FL 33620.

II. System Equation Formulation: Part I

Consider systems which have network models consisting of interconnections of linear distributed elements (e.g., TEM transmission lines, waveguides), lumped linear or nonlinear elements, dependent sources, and independent sources. Partition the network into two parts as shown in Fig. 1. One part consists of linear (distributed and/or lumped) elements. The other part contains any lumped nonlinear or time-varying elements and independent sources.

Silverberg's [3] procedure is to solve for the terminal behavior of the linear part of the network in the frequency domain and then convert to a terminal time-domain description by numerical inverse-transform techniques. The time-domain solution for the whole network is obtained step-by-step in time at the interface of the two parts, by a simultaneous solution of a convolution equation representing the linear part with a differential equation representing the nonlinear part. The simultaneous solution is accomplished at each time increment by solving algebraic equations obtained by application of the trapezoidal integration rule to the original equations.

For the moment let us focus our attention on the linear part of the network. Wouldn't it be nice if the frequency-

0018-9480/79/1100-0890$00.75 ©1979 IEEE